



# A multi-pollutant and multi-sectorial approach to screening the consistency of emission inventories

Philippe Thunis<sup>1</sup>, Alain Clappier<sup>2</sup>, Enrico Pisoni<sup>1</sup>, Bertrand Bessagnet<sup>1</sup>, Jeroen Kuenen<sup>3</sup>, Marc Guevara<sup>4</sup>, and Susana Lopez-Aparicio<sup>5</sup>

<sup>1</sup>European Commission, Joint Research Centre, Ispra, Italy

<sup>2</sup>Université de Strasbourg, Laboratoire Image Ville Environnement, Strasbourg, France

<sup>3</sup>TNO, Department of Air, Climate and Sustainability, Utrecht, the Netherlands

<sup>4</sup>Barcelona Supercomputing Center, Barcelona, Spain

<sup>5</sup>NILU – Norwegian Institute for Air Research, 2027 Kjeller, Norway

**Correspondence:** Philippe Thunis (philippe.thunis@ec.europa.eu)

Received: 22 November 2021 – Discussion started: 16 December 2021

Revised: 31 May 2022 – Accepted: 16 June 2022 – Published: 8 July 2022

**Abstract.** Some studies show that significant uncertainties affect emission inventories, which may impeach conclusions based on air-quality model results. These uncertainties result from the need to compile a wide variety of information to estimate an emission inventory. In this work, we propose and discuss a screening method to compare two emission inventories, with the overall goal of improving the quality of emission inventories by feeding back the results of the screening to inventory compilers who can check the inconsistencies found and, where applicable, resolve errors. The method targets three different aspects: (1) the total emissions assigned to a series of large geographical areas, countries in our application; (2) the way these country total emissions are shared in terms of sector of activity; and (3) the way inventories spatially distribute emissions from countries to smaller areas, cities in our application. The first step of the screening approach consists of sorting the data and keeping only emission contributions that are relevant enough. In a second step, the method identifies, among those significant differences, the most important ones that provide evidence of methodological divergence and/or errors that can be found and resolved in at least one of the inventories. The approach has been used to compare two versions of the CAMS-REG European-scale inventory over 150 cities in Europe for selected activity sectors. Among the 4500 screened pollutant sectors, about 450 were kept as relevant, among which 46 showed inconsistencies. The analysis indicated that these inconsistencies arose almost equally from large-scale reporting

and spatial distribution differences. They mostly affect SO<sub>2</sub> and PM coarse emissions from the industrial and residential sectors. The screening approach is general and can be used for other types of applications related to emission inventories.

## 1 Introduction

Air pollution remains a critical issue, as it is one of the main causes of human health damage worldwide. In the EU28 alone, exposure to a pollutant such as fine particulate matter (PM<sub>2.5</sub>) is estimated to be responsible for approximately 390 000 premature deaths per year (EEA, 2020). Reducing pollution levels requires appropriate regulatory decisions leading to the implementation of effective abatement strategies. Such decisions are not easy to support because they may involve several pollution sources interacting through complex and non-linear atmospheric phenomena. As only models can simulate the impacts of emission reductions considering the complexity of the atmosphere, they are potentially the only tools able to support the planning of reduction strategies. The accuracy of their results, however, strongly depends on the quality of a wide range of input data (meteorological fields, boundary conditions, land use data, and pollutant emissions; Im et al., 2018; Zhu et al., 2019; Dufour et al., 2021; de Meij et al., 2009, 2018; Cuvelier et al., 2007; Thunis et al., 2007). Many previous studies have shown that emis-

sions are an input with one of the most critical influences on the results of air-quality modeling and, in particular, on the urban-scale source apportionment used to design air-quality plans (Kryza et al., 2015; Zhang et al., 2015). More alarmingly, some studies have shown that significant uncertainties affect emission inventories, which may impeach conclusions based on air-quality model results (Trombetti et al., 2018; Markakis et al., 2015). These uncertainties result from the need to compile a wide variety of information to develop an emission inventory. Indeed, these inventories are prepared for many pollutants ( $\text{NO}_x$ , PM, NMVOC (non-methane volatile organic compounds),  $\text{SO}_2$ , CO,  $\text{CO}_2$ , etc.) and for many activity sectors (transport, industry, residential, agriculture, natural sources, etc.) that entail different emission processes. The spatial and temporal distribution of emissions is typically based on proxies that can be estimated by very different methods. For example, top-down approaches start from emission estimates at a large scale (e.g., a national inventory) and disaggregate spatially and temporally the emissions with finer-scale proxies. Bottom-up approaches compute the emissions directly, starting from local spatial and temporal proxies based on accurate locations or high-resolution shape patterns (road, ship routes, high-resolution land use, vehicle counting, etc.). Various sources of proxies are reported to create very-high-resolution inventories at the urban scale (Zheng et al., 2021; Geng et al., 2017; Ramacher et al., 2021). One of the most important challenges in compiling local-scale emission inventories is remaining consistent with data provided by national inventories while providing satisfactory accuracy at all locations and times. For all these reasons, compiling emission inventories can lead to different results depending on the methods and data used.

In previous work, Thunis et al. (2016) proposed a methodology to compare two emission estimates over a given area based on a limited input, i.e., the total emission per pollutant and macro-sector. With this method, the differences between the total emissions of the two inventories are apportioned in terms of emission factors and activity differences. This information can then be used by emission inventory developers to identify the main causes for these discrepancies and likely errors in their estimates. However, this method is able to apportion differences between emission factors and activity only when the difference in emission factors is known for at least one of the emitted pollutants. Since this led to arbitrary treatment of one pollutant, Clappier and Thunis (2020) improved the method by implementing a probabilistic approach to find the most likely allocation between emission factor and activity to remove this limiting assumption. In their work, Trombetti et al. (2018) then extended the approach to multiple inventories.

While the proposed approach shares some aspects of graphical representation with the previous method, it differs in terms of diagnostics. The three original features of the new approach are: (1) differences in total emissions are allocated to three key components that provide information on the sec-

toral and spatial shares of the emissions at two geographical scales for each pollutant; (2) the ability to perform the analysis simultaneously for a large number of locations, while systemically excluding emissions that are not relevant (lower emissions compared to others); and (3) to rank the largest inconsistencies between the two inventories.

This new method can be applied to two inventories, which may be either two versions or two different years of a given inventory; two inventories based on distinct sources of information, e.g. CAMS-REG (Kuenen et al., 2022) and EDGAR (Crippa et al., 2018); top-down vs. bottom-up approaches; regional vs. Europe wide; etc. Here, we illustrate the use of the proposed method by focusing on comparisons between two versions of the same inventory, and apply the screening methodology to a continental-scale inventory used to compile air-quality modeling at the urban scale, i.e., the CAMS-REG inventory (Kuenen et al., 2022). In a follow-up paper, we extend and apply the approach to the comparison of different inventories.

The paper starts with a description of the screening approach that includes its required input data, the methodology itself, and its output. An application with the EU-wide CAMS-REG inventory is then presented in Sect. 3, while further considerations are addressed in Sect. 4.

## 2 The screening approach

The approach presented in this article aims to compare two emission inventories over a series of geographical areas within the domain they spatially cover. These geographical areas include two groups characterized by different scales: large (e.g., country) and focal (e.g., cities) areas. For each pollutant, the method screens the consistency of the inventories in terms of three aspects: (1) the total pollutant emissions assigned at large scale; (2) the way these total pollutant emissions are shared in terms of sector of activity; and (3) the way large-scale emissions are distributed to the focal areas.

In other words, the screening approach intends to answer the following questions:

- Are there inconsistencies in total pollutant emissions at a large-scale level?
- Are there inconsistencies in the sectoral contributions to the emissions at a large-scale level?
- Are there inconsistencies in the way inventories distribute large-scale emissions spatially?

Note that the method proposed here is designed with a focus on the spatial dimension. Other uncertainties related to emission inventories (e.g., speciation of VOC or PM, temporal distribution of the emissions) are not considered.

### 2.1 Input data

Based on a  $0.1 \times 0.1^\circ$  gridded emission inventory detailed in terms of emitted pollutants (denoted as “p”) and sectors of activity (denoted as “s”), the data required for each pollutant and sector (denoted as a [p, s] couple) are twofold and consist of:

- Emission totals aggregated over specific areas of interest (e.g., urban areas, agriculture-intensive areas, industrial areas, etc.). These areas, referred to as *focal areas*, can be freely selected and represent locations where we wish to assess the consistency of the inventory. The associated emissions are denoted by a lowercase notation  $e_{p,s}$ .
- Emission totals aggregated over larger areas (e.g., country, regions, modeling domains, etc.). In general, these areas correspond to the larger scale at which data are reported. For example, “country” is the scale of interest for EU-wide inventories, as this is the scale at which national emission totals are typically reported or estimated. These areas are referred to as *larger-scale areas* and their emissions denoted by an uppercase notation  $E_{p,s}$ .

The number of focal areas is denoted by  $N$ . We will also denote sectorial emission totals by an overbar ( $\bar{E}_p = \sum_s E_{p,s}$ ).

### 2.2 Methodology

The number of [p, s] points under screening is equal to the product of the number of pollutants and the number of sectors multiplied by the number of focal areas (i.e.,  $N \times N_p \times N_s$ ). Because this number may become overwhelming, we proceed with a number of steps that help to focus the screening on priority aspects. To this end, threshold parameters are set first to restrict the screening to relevant emissions (i.e., emissions that are large enough), and second to prioritize these relevant inconsistencies according to their magnitude. These steps, schematically represented in the flowchart of Fig. 1, are discussed in the next sub-sections.

#### 2.2.1 Exclusion of non-relevant emissions

Not all emission data ( $E$  and  $e$  for all pollutants and sectors) are kept for the analysis. Emissions that are smaller for a given pollutant and sector are disregarded, even though differences might be large between emission estimates for those emissions. For the exclusion, we proceed as follows: for each [p, s] and each inventory, we calculate the ratio between the focal area emission ( $e_{p,s}$ ) and its respective larger-scale pollutant total, i.e.,  $\bar{E}_p$ :

$$X_{p,s} = \max_{\{inv\}} \frac{e_{p,s}}{E_p} \tag{1}$$

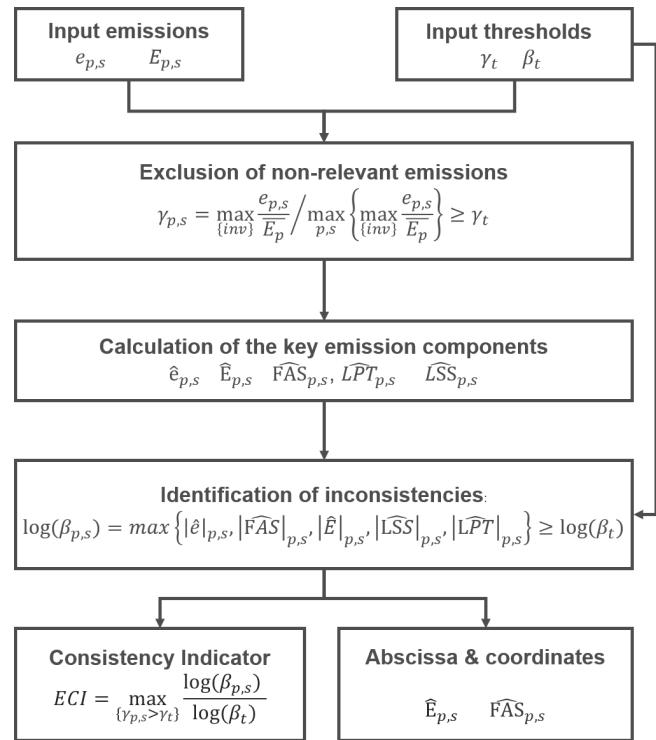


**Figure 1.** Flowchart of the steps to screen emission inventories. See details in the text.

For each [p, s] couple, the maximum values of the two inventories is then normalized by the maximum obtained over all [p, s] and over the two inventories for a given focal area:

$$\gamma_{p,s} = \frac{X_{p,s}}{\max_{p,s} \{X_{p,s}\}} \tag{2}$$

This final ratio informs on the relative importance of each [p, s] couple. Then, [p, s] couples are excluded from the analysis when this ratio is below a given threshold value  $\gamma_t$  (arbitrary input). The purpose of this scaling is to avoid flagging issues for emissions that are proportionally less relevant. Rewriting Eq. (1) as  $X_{p,s} = \max_{\{inv\}} \frac{e_{p,s}}{E_p} \frac{E_p}{e_p}$ , we see that we exclude from the analysis

1. sectorial activities that have a low share over focal areas (low  $\frac{e_{p,s}}{E_p}$ ), e.g., NMVOC emissions in the power plants sector, and/or
2. emissions for pollutants that have a low urban share (low  $\frac{E_p}{e_p}$ ), e.g., agriculture.

As we will see in the application (Sect. 3), this exclusion step leads to elimination of a large majority of the [p, s] couples from the screening process (between 80 % and 90 %).

**2.2.2 Decomposition into key components**

The objective of the decomposition is to isolate emission characteristics that are associated with the inventory compilation process, in order to facilitate resolution of the detected inconsistencies. The three main characteristics are (1) the pollutant totals over large areas (LPT), the sectorial shares over large areas (LSS), and the activity share over the focal areas (FAS). To isolate these components, we decompose the ratio of the known pollutant-sector emissions for each focal areas as follows:

$$\frac{e_{p,s}^1}{e_{p,s}^2} = \frac{\frac{e_{p,s}^1}{E_{p,s}^1}}{\frac{e_{p,s}^2}{E_{p,s}^2}} \cdot \frac{\frac{E_{p,s}^1}{E_p^1}}{\frac{E_{p,s}^2}{E_p^2}} \cdot \frac{E_p^1}{E_p^2}, \tag{3}$$

where  $\bar{E}_p$  represents the larger-scale emissions summed over all sectors for a given pollutant. Superscripts refer to the two inventories used for the screening. Equation (3) is an identity where all terms are known from input quantities, i.e., the focus and larger-scale emissions detailed in terms of pollutants and sectors. The three terms on the right-hand side of the identity provide information on FAS, LSS, and LPT, respectively.

For convenience, we rewrite Eq. (3) in logarithm form as

$$\log\left(\frac{e_{p,s}^1}{e_{p,s}^2}\right) = \log\left(\frac{\frac{e_{p,s}^1}{E_{p,s}^1}}{\frac{e_{p,s}^2}{E_{p,s}^2}}\right) + \log\left(\frac{\frac{E_{p,s}^1}{E_p^1}}{\frac{E_{p,s}^2}{E_p^2}}\right) + \log\left(\frac{E_p^1}{E_p^2}\right), \tag{4}$$

which can be rewritten as Eq. (5) with simplified notations:

$$\hat{e} = \widehat{FAS} + \widehat{LSS} + \widehat{LPT}, \tag{5}$$

where the hat symbol indicates that quantities are expressed as logarithmic ratios. These three quantities are at the basis of the screening methodology and serve as input for the graphical representation as well.

**2.2.3 Identification of inconsistencies**

One of the main steps of the methodology consists of keeping only the largest differences among the relevant emissions identified in Sect. 2.2.1. The comparison of two emission inventories always leads to different estimates, as inventories can be calculated by different methods (e.g., different activity data, emission factors, and spatial disaggregation to the grid).

Differences originate from methodological choices but also from errors generated during the inventory compilation process. When differences are small, it is not possible to tell whether they originate from methodological choices or from errors. Moreover, it is not possible to assess whether one methodological choice leads to an improvement as compared to the other, because true emissions remain unknown (Kryza

et al., 2015). We will refer to these small differences as “uncertainty”.

Although very large differences may result from methodological choices as well (e.g., inclusion or non-inclusion of condensable emissions for the residential sector), they are more likely to be associated with errors. Given the magnitude of the differences, it will, in most cases, be possible to identify one best value out of the two inventory estimates, even though the truth is unknown. These large differences therefore point to a list of potential issues for inventory compilers to check and fix where applicable, opening the path to potential improvement. In this work, these large differences are termed “inconsistencies” and are intended as differences that are large enough to ensure that one of the two inventory values is tenable (i.e., justifiable), whereas the other is not.

In the proposed screening methodology, a threshold is introduced to distinguish inconsistencies from uncertainties. This arbitrary level is denoted as  $\beta_t$  and represents free input data in this screening process.

The detection of inconsistencies is performed as follows: for each [p, s], we check that neither of the two input data –  $|\hat{E}|$  and  $|\hat{e}|$  – exceed the threshold, but also that none of the three main components –  $|\widehat{FAS}|$ ,  $|\widehat{LSS}|$ , and  $|\widehat{LPT}|$  – do either. This is to flag potential compensating effects between  $\widehat{FAS}$  and  $\hat{E}$ , since  $\hat{e} = \widehat{FAS} + \hat{E}$ , and between  $\widehat{LPT}$  and  $\widehat{LSS}$ , since  $\hat{E} = \widehat{LPT} + \widehat{LSS}$ . To achieve this, the following indicator is defined:

$$\log(\beta_{p,s}) = \max\left\{|\hat{e}|_{p,s}, |\widehat{FAS}|_{p,s}, |\hat{E}|_{p,s}, |\widehat{LSS}|_{p,s}, |\widehat{LPT}|_{p,s}\right\}. \tag{6}$$

Differences beyond the threshold ( $\beta_{p,s} \geq \beta_t$ ) are then flagged as inconsistencies.

**2.2.4 Calculation of an emission consistency indicator**

As a follow-up step, all [p, s] couples that remain after the relevance- ( $\gamma_{p,s} > \gamma_t$ ) and inconsistency-detection steps ( $\beta_{p,s} > \beta_t$ ) are used to calculate an emission consistency indicator (ECI) as follows:

$$ECI = \max_{\{\gamma_{p,s} > \gamma_t\}} \frac{\log(\beta_{p,s})}{\log(\beta_t)}. \tag{7}$$

The ECI quantifies the maximum difference among all relevant [p, s], normalized by the inconsistency level ( $\beta_t$ ). It therefore quantifies the ratio between the maximum inconsistency and the assumed level of uncertainty. A value of ECI less than one means that all differences are considered as uncertainty (in other words, none of the inventory can be identified as best performing). Together with the ECI, which quantifies this maximum difference, we associate the percentage of inconsistent [p, s] with respect to the total amount of relevant data, to provide information on the number of

detected inconsistencies. To facilitate the screening process, these concepts are displayed graphically. This is discussed in Sect. 2.3.

### 2.3 Graphical display

#### 2.3.1 Diamond diagram

For the graphical representation, we use an aggregated form of Eq. (5), recalling that the two last terms on the right-hand side combine into the ratio of the larger-scale [p, s] emissions, i.e.,

$$\hat{e} = \widehat{FAS} + \hat{E}, \tag{8}$$

where FAS is related to the large-scale-to-focus-scale emission share and E is related to the large-scale emissions. Equation (8) is the basis of the “diamond” diagram (Fig. 2) that provides an overview of all inconsistencies detected during the screening process. In this diagram, each inconsistent emission [p, s] is represented by a point that has larger-scale emissions ( $\hat{E}$ ) as abscissa and focus activity share as ordinate ( $\widehat{FAS}$ ). The sum of these two terms ( $\hat{e}$ ) is equal for points that lie on “−1” slope diagonals. At this stage it is important to note that positive differences in terms of larger-scale emissions and focal area shares will characterize points lying on the right and top parts of the diagram, respectively. In addition, the upper-right and lower-left diagram areas indicate summing-up effects, whereas the lower-right and top-left areas highlight compensating effects.

The diamond shape (in the middle of the diagram) derives from Eq. (8), where the  $\beta_t$  threshold is used to draw the inconsistency limit for each of its three terms. Each [p, s] point lying outside this shape is therefore characterized by an inconsistency in terms of either E, FAS, or/and e, small or large according to its relative position in the diagram. The calculation of the inconsistency limit (Eq. 6), however, considers LPT and LSS as two additional criteria. Because of their link ( $\hat{E} = \widehat{LPT} + \widehat{LSS}$ ), a point within the diamond therefore represents an inconsistency in terms of LPT and LSS that compensate each other, since their sum remains lower than the threshold ( $\hat{E} \leq \log(\beta_t)$ ; otherwise, the point would lie outside the diamond). We recall that LPT is related to the total of the large-scale emissions, whereas LSS provides information on their sectoral share.

In this diamond diagram, shapes are used to differentiate activity sectors, while colors differentiate pollutants. The size of the symbol is proportional to the relevance of the emission contribution ( $\gamma$ ). Finally, we use symbol filling to distinguish priorities among inconsistencies related to the three components, LPT, LSS, and FAS. The priority is set as follows: 1–LPT, 2–LSS, and 3–FAS. This is motivated by the fact that larger-scale inconsistencies are easier to tackle and might correct for many focal area inconsistencies at the same time (i.e., for all focal areas belonging to a given larger area). The priority is then set by checking, in this order, whether the

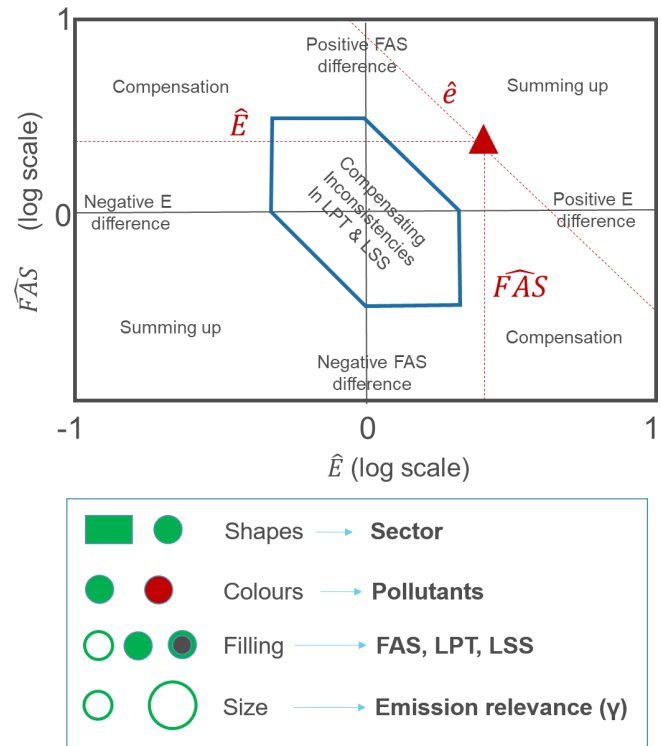


**Figure 2.** Diamond diagram and representation of the codification. LPT provides information on the total of the large scale emissions, LSS on their sectoral share, FAS on the large-to-focus scale share and E on the large scale emissions

component exceeds the threshold or is larger than the remaining components. In practice, this is implemented as follows:

1. If  $\widehat{LPT} \geq \log(\beta_t)$  or  $\widehat{LPT} \geq \max[\widehat{FAS}, \widehat{LSS}]$ , then priority is set to the larger-scale pollutant total (LPT).
2. If step 1 is not fulfilled and if  $\widehat{CSS} \geq \log(\beta_t)$  or  $\widehat{CSS} \geq \widehat{UAS}$ , then priority is set to the larger-scale sectorial share (CSS).
3. If neither of steps 1 and 2 are fulfilled, priority is set to the focal area activity share (FAS).

Note that compared to the emission diagram proposed by Thunis et al. (2016) and Clappier and Thunis (2020), the diagram proposed here does not distinguish between acceptable (within the diamond) and non-acceptable data (outside the diamond), but displays only inconsistencies (i.e., data to be checked for which some explanation must be found). Moreover, the current formulation does not rely on probabilistic assumptions and directly relates to emission characteristics that are readily available to emission developers.

#### 2.3.2 Supporting diagrams

In addition to the diamond diagram, other diagrams are proposed to support the interpretation of the screening. These

diagrams are designed to provide additional information by detailing further some aspects (e.g., geographical) at the expenses of aggregation or simplification (e.g., limitation to top inconsistencies) of other aspects. These diagrams are

- *Overview map.* Data are displayed on a geographical map to easily identify the inconsistencies for each focal area. However, only the maximum inconsistency ( $\max\{\beta\}$ ) for each focal area is shown. While the size is here proportional to the magnitude of the inconsistency, the symbol shapes, colors, and filling remain similar to the overview diamond.
- *Bar chart.* For a given pollutant and focal area, this diagram allows visualization of inventory differences directly in terms of FAS, LSS, and LPT components. This diagram is used here as validation means (with respect to the diamond results).

We discuss these visualizations further in the Sect. 3, with a graphical example and comments for each type of plot.

### 3 Application

#### 3.1 Input

In this section, we apply our screening methodology to the CAMS-REG regional anthropogenic emission inventory that covers emissions for United Nations Economic Commission for Europe (UNECE) for the main air pollutants and greenhouse gases (Kuenen et al., 2022). The method starts from the emissions reported by European countries to the United Nations Framework Convention on Climate Change (UNFCCC) (for greenhouse gases) and to the European Monitoring and Evaluation Programme (EMEP) and the Centre on Emission Inventories and Projections (CEIP) (for air pollutants), which have been aggregated into 246 different combinations of sectors and fuels. Reported data are analyzed by sector and completed with alternative emission estimates, where the completeness, consistency, and/or quality of the reported data was not sufficiently accurate. In practice, reported data were found fit for purpose for EU member states and the UK, Norway, Iceland, and Switzerland, while for other countries, alternative emission estimates were used. In addition, some further modifications were made to the dataset for which we refer to Kuenen et al. (2022). This results in a complete emission inventory for all countries, which is then spatially distributed at high resolution using a consistent methodology over the whole domain.

For the comparison presented in this paper, we use two versions of the CAMS-REG inventory for the same year, i.e., 2015:

- CAMS-REG v2.2.1: a version covering the years 2000–2015, based on the official reported data of air pollutants and greenhouse gases in the year 2017.

- CAMS-REG v4.2: this version covers the years 2000–2017, based on the official reported data of air pollutants and greenhouse gases in the year 2019.

In comparison to version 2.2.1, the methodology for the total emissions by country, pollutant, sector, and year in CAMS-REG-v4.2 is largely similar; however, the difference in reporting year of emissions may introduce substantial differences in sectoral or country total emissions in specific cases. This happens since official country emission data are reported on an annual basis for all historical years, which implies that emissions for the year 2015 have been reported annually since 2017. Inventories are continuously improved by means of updating methodologies (new activity data, new emission factors, etc.), which implies that historical emissions from a single year (2015 in this case) are different in each reporting year. On the other hand, some of the changes are the result of methodological changes in the CAMS-REG inventory, which are mainly related to the spatial distribution, where CAMS-REG-v4.2 contains, among other things, an improved split in road transport emissions between urban, rural, and highway shares, and agriculture (new proxies for manure spreading, fertilizer application based on the JRC CAPRI model; Britz and Witzke, 2015). It also uses a new approach for agricultural waste burning, improves the point-source database, and uses updated harmonized inland and sea shipping based on the FMI STEAM model (Jalkanen et al., 2009). Further details on these changes are provided in Kuenen et al. (2022).

It is important to stress that the proposed screening methodology assesses the overall consistency of the two inventory versions, i.e., it covers the consistency of the inventory compilation itself but also the consistency of its input data (in this case, country-reported emissions).

Focal areas are defined as the functional urban areas (FUA; OECD 2012) for which emissions ( $e_{p,s}$ ) are obtained by aggregating grid cell values. The FUA is composed of a core city plus their wider commuting zone, consisting of the surrounding travel-to-work areas. As depicted by blue shading in Fig. 3, 150 FUAs across Europe were selected for this screening. Details on these cities are provided in Thunis et al. (2018). The larger-scale emissions ( $E_{p,s}$ ) are defined at country level, the level at which CAMS-REG takes the official reported data as input.

In terms of pollutants,  $E_{p,s}$  and  $e_{p,s}$  include the following:  $\text{NO}_x$ , NMVOC,  $\text{PM}_{2.5}$ ,  $\text{PM}_{\text{CO}}$  (coarse PM, calculated as the difference between  $\text{PM}_{10}$  and  $\text{PM}_{2.5}$  emissions from CAMS-REG),  $\text{SO}_2$ , and  $\text{NH}_3$ , whereas sectors are based on the Gridded Nomenclature For Reporting (GNFR) classification. The original GNFR sectors have been aggregated in five categories: road transport (F), residential (C), power plants (A), industry (B), and others (D, E, I, J). The latter category includes waste, fugitive emissions, solvents, and off-road transport. As we focus on urban areas, agriculture emissions (K, L) are not relevant and therefore not included in the analysis.

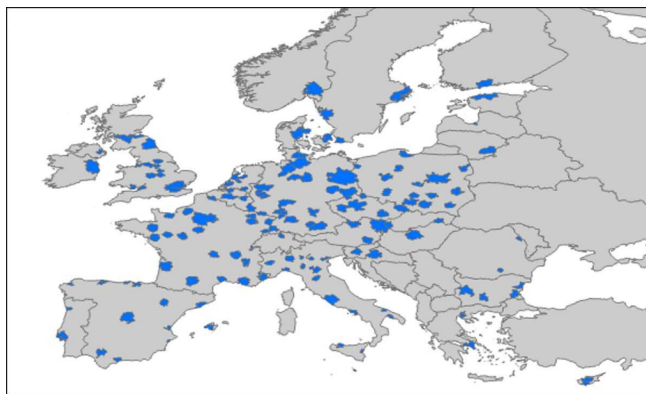


**Figure 3.** Map of the functional urban areas (FUA) considered for the emission screening.

Shipping (G) and air transport (H) are also not part of the analysis.

For this inventory, LPT concerns the country-level total emissions, LSS the sectoral total emissions at country level, and FAS the sectoral emissions at the local level (city of interest). Note that the selection of the large-scale and focal areas, as well as of the sectors to consider, is a free user choice.

Finally, the relevance and inconsistency thresholds are set in this work to  $\gamma_t = 0.5$  and  $\beta_t = 2$ . Although the choice of these threshold values is arbitrary and may seem challenging, this is not the case in practice, and identifying the inconsistencies is a robust process. A too low threshold will lead to detecting too many differences among which the smallest (at the uncertainty level) do not allow assessment of what is best. However, the largest differences (inconsistencies) are identified and can be taken care of to improve one or both inventories. A too low threshold will therefore lead to confusing information by mixing uncertainties and inconsistencies. On the other hand, a too high threshold will lead to detecting too few inconsistencies and, therefore, to missing errors that could potentially be corrected. In practice, it is recommended to start with a high threshold and lower it progressively until differences can no longer be justified. The values for the relevance and inconsistency thresholds ( $\gamma_t$  and  $\beta_t$ ) presented here reflect these considerations.

### 3.2 Results

The diamond diagram (Fig. 4) displays the inconsistencies between the CAMS-REG-v2.2.1 and v4.2 inventories over the entire emission domain, i.e., Europe. Among the 4500 screened [p, s] points, corresponding to the product of 150 cities per 6 pollutants and 5 sectors, only about 450 were kept after application of the relevance threshold ( $\gamma \geq 0.5$ ). Among the remaining 450 points, 46 show inconsistencies ( $\beta > 2$ ) as indicated by the lower-right number (NI). In other terms, about 9 % of the relevant [p, s] show inconsistent values (number associated in brackets) aside the ECI. In our ap-

plication, the ECI is about a factor 70, meaning that the maximum inconsistency is about 70 times larger than the assumed level of uncertainty.

The summary table at the bottom of the diagram supports the interpretation by ranking inconsistencies in terms of pollutant, sector, and type (FAS vs. LSS vs. LPT). Most of the inconsistencies arise for  $\text{SO}_2$  (13) and  $\text{PM}_{\text{CO}}$  (16), primarily from the industrial and residential sectors, and originate both from the country ( $\text{LPT} + \text{LSS} = 2 + 22$ ) and local scales ( $\text{FAS} = 22$ ). It is worth noting that few inconsistencies are within the diamond, pointing to a limited number of compensations between LPT and LSS large-scale inconsistencies (i.e., overestimation in terms of pollutant total compensated by an underestimation in terms of sectorial share, and vice versa). This information is graphically detailed by representing the [p, s] points with varying colors and symbols.  $\text{PM}_{\text{CO}}$  inconsistencies are important in magnitude and are mainly related to lower estimates (points are below the  $x$ -axis) by v4.2 of the urban share (points are distributed along a vertical line). It is interesting to note that points are mostly distributed either on a vertical or horizontal line, indicating the absence of compensation (top-right and bottom-left parts of the diagram) or summing-up effects (top-right and bottom-left parts of the diagram).

The European map presented in Fig. 5 flags out the inconsistency that dominates in each city. It is interesting to note that while the total number of inconsistencies (46) might seem large, the map shows that in some countries, the same type of inconsistency is widespread. This is the case for the  $\text{PM}_{\text{CO}}$  industrial emissions in the UK, the  $\text{SO}_2$  industrial emissions in France, or for the NMVOC residential emissions in the Czech Republic. As the size of the symbol is here proportional to the magnitude of the inconsistency, the  $\text{PM}_{\text{CO}}$  emissions from the industrial sector might need a priority check in some UK cities. Even though these inconsistencies appear in different countries, their type is similar, and resolving one might bring useful information to resolve the others.

We focus now on some of these inconsistencies and try to understand their origin. Examples are picked among those showing important inconsistencies, with the aim of illustrating different types of inconsistencies, i.e., in terms of LSS, FAS, and LPT (Fig. 6). Note that depending on pollutant and sector, the ECI can differ quite strongly in magnitude, explaining the different range of values in our examples.

- *Vilnius: inconsistent country totals for  $\text{PM}_{2.5}$ .* In Vilnius (Lithuania), the ECI is about 2 (see diamond plot in Fig. 6, top row), indicating inconsistencies that are about twice as large as the level of uncertainty. The flagged inconsistency is aligned along the  $x$ -axis, indicating issues in terms of country  $\text{PM}_{2.5}$  values, in particular pollutant levels (LPT). The associated bar chart highlights a factor 2 to 3 difference between the CAMS-REG-v2.2.1 and v4.2 estimates (Fig. 6). Note that the

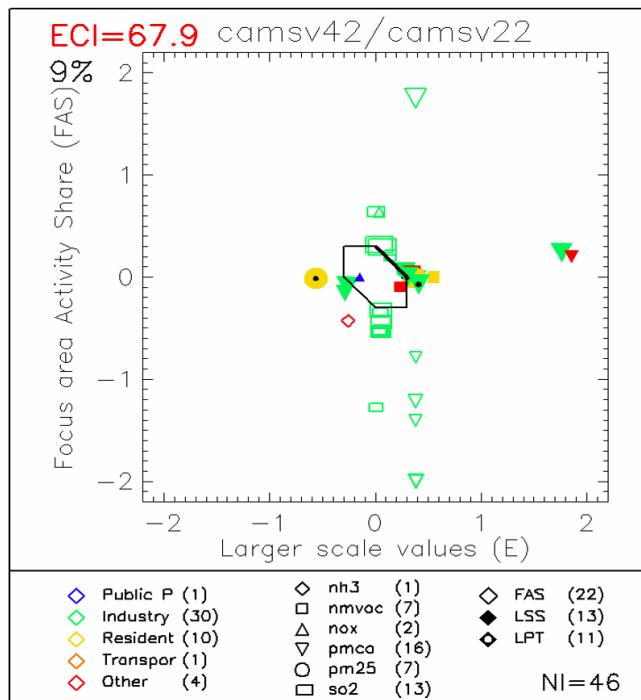


**Figure 4.** Overview diamond. Symbols and colors are used to distinguish pollutants and sectors, respectively. The  $x$ - and  $y$ -axes indicate inconsistencies in country emissions ( $\hat{E}$ ) and urban share ( $\hat{FAS}$ ), respectively, while the overview table provides information on the origin of the inconsistencies in terms of sector, pollutant, and country/city scale (FAS, LSS, LPT). The ECI indicator indicates the ratio between the magnitude of the maximum inconsistency and the assumed level of uncertainty ( $\beta$ ). The percentage number indicates the fraction of inconsistencies ( $\beta \geq \beta_t$ ) among the relevant emissions ( $\gamma \geq \gamma_t$ ). See additional explanations in the text.

country sectorial shares also diverge for the industrial and transport sectors. This is, however, seen by the screening tool as a secondary priority.

The changes can be explained by the changes in the emission reporting that is used as input to the CAMS-REG inventories. Significant updates were made in the 2019 submission compared to the 2017 submission for Lithuania. For example,  $PM_{2.5}$  emissions from the residential sector decreased by almost a factor 4, whereas road transport emissions increased by  $\sim 70\%$ . National total  $PM_{2.5}$  emissions reported by Lithuania for 2015 were reduced by more than 50% between submissions in 2017 and 2019.

- *Dublin: inconsistent industry country share for  $PM_{2.5}$ .* In Dublin, the ECI is about 50, indicating inconsistencies that are about 50 times larger than the level of uncertainty. The flagged inconsistency ( $PM_{CO}$  from industry) lies on the right, indicating a much larger value attributed to this pollutant and sector in the CAMS-REG-v4.2 version. This is confirmed in the associated bar

chart (Fig. 6, second row), which highlights a totally different industrial share in the two inventories. This country-scale issue is partly echoed in the urban share, but this is seen by the screening tool as a secondary priority. Similar to the Vilnius case above, this can be explained by changes in country reporting. Whereas total emissions in the 2017 submission for industry were 1.5 kt  $PM_{2.5}$  and 1.6 kt  $PM_{10}$ , in the 2019 submission, the  $PM_{2.5}$  emissions amounted to 1.9 kt and  $PM_{10}$  emissions were 7.7 kt. Hence,  $PM_{CO}$  emissions from industrial sources were increased by more than a factor 50, from 0.1 to 5.8 kt, between the versions.

- *Newcastle: inconsistent industry urban share for  $PM_{CO}$ .* In Newcastle (UK), the ECI is 68 (Fig. 6, third row), indicating inconsistencies that are about 70 times larger than the level of uncertainty. The flagged inconsistency ( $PM_{CO}$  from industry) is mostly driven by the urban share, but country values differ greatly as well (factor 2). Note that large differences of the same type also occur for  $PM_{2.5}$ . While this is not flagged as a major inconsistency by the screening approach (because the relative importance of the emissions ( $\gamma$ ) is too small), this might become the case when the  $PM_{CO}$  inconsistency has been resolved. The associated bar chart highlights differences in country totals and country sectorial shares, but these are not sufficient (in terms of  $\gamma$  or  $\beta$ ) to trigger flagging. On the contrary, the very large difference in the urban share, with CAMS-REG-v4.2 exceeding v2.2 emissions by almost a factor 100, is flagged. As mentioned above, this inconsistency is present in many UK cities. The inconsistency can be explained partly by changes in reporting between 2017 and 2019 submissions, as the  $PM_{CO}$  from industry increased from 15.8 to 35.2 kt. For the distribution in the country, the European Pollutant Release and Transfer Register (E-PRTR) is used for distributing emissions to point-source installations. When checking in detail for this location, a factor-1000 error in E-PRTR reporting was found, which led to an over-allocation of PM emissions from the industrial sector to this specific industrial site located within the Newcastle urban area. This means that in CAMS-REG-v4.2, emissions in this particular location are overestimated, which is compensated for by underestimated emissions elsewhere in the UK.
- *London: inconsistent “other” urban share for  $NH_3$ .* In London (UK), the ECI is 2.5, indicating inconsistencies that are about 2.5 times larger than the level of uncertainty (Fig. 6, bottom row). The flagged inconsistency ( $NH_3$  from the “other” sector) results from both urban and country differences that add up, but the dominating factor is the urban share. The associated bar chart confirms this issue, while differences in country totals and country sectorial shares appear moderate in comparison

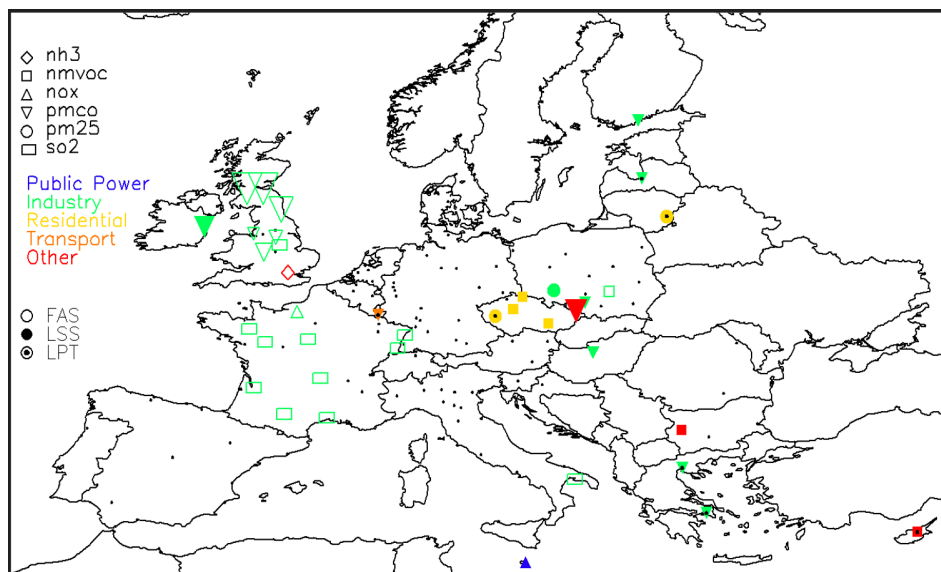


**Figure 5.** EU (overview) map. Only cities where at least one [p, s] couple ratio with relevant emissions ( $\gamma \geq \gamma_i$ ) is above the inconsistency threshold ( $\beta \geq \beta_i$ ) are shown by a symbol. If more than one [p, s] fulfills these two conditions, only the largest is shown. For all others, cities are represented by a black dot.

to the urban share issue. In contrast to Newcastle, this issue only appears for London.

In this specific case, it was found that a relatively large proportion of  $\text{NH}_3$  emissions was reported in the category “other waste” for the UK as a whole. Given the relatively low importance of the sector “other waste” and the absence of point-source information for  $\text{NH}_3$  for this particular sector, these emissions were allocated using a surrogate point-source distribution, where all emissions ended up in the same point source in London, thus significantly over-allocating emissions in this location. This therefore points to an inconsistency in the CAMS-REG methodology.

Half of the inconsistencies between the two versions of CAMS-REG considered in this study can be attributed to changes in country reporting. All European countries annually revise and report their historical annual emissions back to 1990; hence, the emissions of, e.g., 2015, are re-reported every year. The differences between the versions may be the result of correction of an error and/or implementation of a different methodology to estimate the emissions. This may be checked in the reports (IIRs) that are submitted annually along with the reported emissions, but likely not all changes are documented in detail. This means that only in a selection of cases will it be possible to define an error in one of the inventories as such, and hence define the better inventory.

An important driver for inventory improvement in recent years has been the annual review of air pollutant inventory data under the NEC directive organized by the European Commission (<https://ec.europa.eu/environment/air/>

reduction/implementation.htm, last access: 1 July 2022), which has led to substantial revisions or nationally reported data since 2017 for all pollutants and sectors.

#### 4 Further considerations

The approach presented in this work is intended as a screening to flag inconsistencies. Only differences that are above a user-defined threshold ( $\beta_i$ ) are detected and smaller differences are disregarded. This threshold reflects the limit between relatively small differences for which no emission inventory can be estimated to be the best (because true emissions are unknown), and differences that are so large that they are likely associated with a large error in one of the two (or both) inventories (hence called inconsistencies), for which it should be possible to identify a best-performing inventory.

While solving a few inconsistencies will generally lower the overall number of inconsistencies, this is, however, not always the case. Indeed, a very large inconsistency can potentially lead to a  $\gamma$  factor that is so large that all other [p, s] for that city would be disregarded in proportion. Once the inconsistency is solved, the new  $\gamma$  estimates might lead to one or more new inconsistencies being flagged. This is therefore a step-wise approach.

The settings used in this work, i.e., the choice of 150 urban areas and the country level as a larger scale, were arbitrarily fixed. The methods allow for flexible choices and could be applied to areas other than urban (e.g., high-emission industrial or intensive agriculture areas) to assess consistency with respect to other types of emissions. Similarly, the larger scale can be adapted to the specific inventory and focus on regions

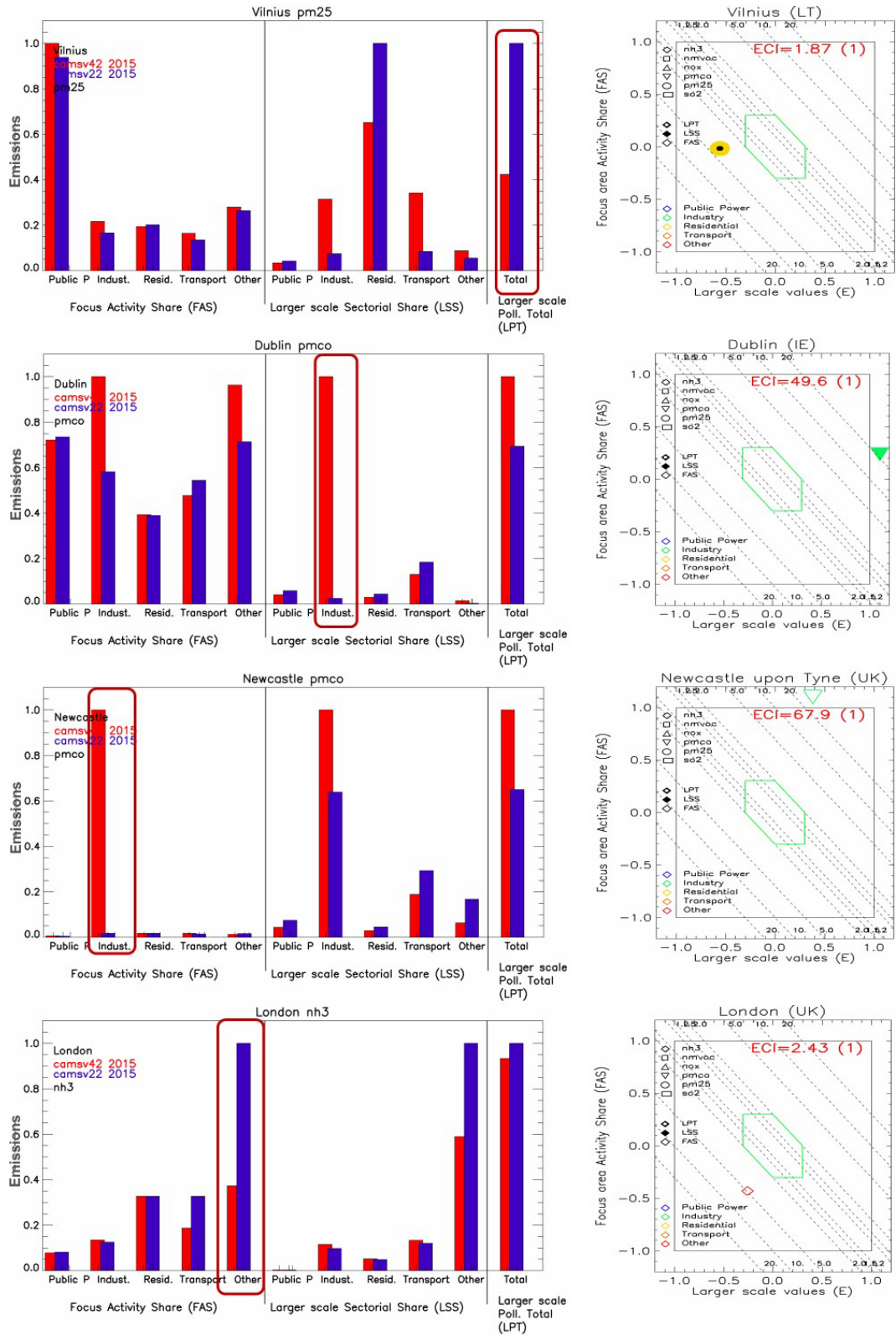


**Figure 6.** Bar charts and city diamond for the cities’ inconsistencies. The bar charts show the values reached for FAS, LSS, and LPT by the two inventories, based on input emission values. Data are graphically scaled relative to the maximum reached for each of the three factors (FAS, LSS, and LPT).

rather than countries, or be defined as the entire modeling domain.

The proposed application focuses on the comparison of two versions of a specific inventory (here, CAMS-REG). Although more challenging, the screening method can be applied to the comparison of two different inventories. Obviously, additional challenges will appear, in particular (1) differences in terms of spatial resolution that might result in sources being excluded from a grid cell for one inventory and included in the other, resulting in artificial differences, or (2) the need for harmonization of the emissions in terms of sectorial categories as a first step before the comparison. This inter-comparison of inventories is the subject of a follow-up paper, where these specific issues are discussed.

Given its flexible settings, the screening method also applies to bottom-up inventories. These can then be compared with themselves (e.g., two versions) or with other inventories. As mentioned earlier, the smaller areas of interest can be designed at own convenience, as is also the case for the larger scale, which, in the extreme case, can be set to the total domain area.

Finally, the screening tool also provides text information that summarizes the inconsistencies by detailing the city, sector, pollutant, type, and amplitude for each. A comment line is associated with each inconsistency, in order to keep track of steps taken to resolve them (or not). A summarizing overview on screening results for the 150 cities is provided in Appendix A.

## 5 Conclusions

In this work, we propose and discuss a screening method to compare two emission inventories. The overall goal is to improve the quality of emission inventories by feeding back the results of the screening to inventory compilers who can check the inconsistencies found and, where applicable, resolve errors. The method targets three different aspects: (1) the total emissions assigned to a series of large geographical areas, countries in our application; (2) the way these country total emissions are shared in terms of sector of activity; and (3) the way inventories spatially distribute emissions from countries to smaller areas, cities in our application. The method provides a way to quantify the level of consistency (intended here as a whole, i.e., emission compilation plus all input-relevant data) between two inventories.

Given the large and possibly overwhelming amount of data to analyze (many pollutants, activity macro-sectors, and cities), the first step of the screening approach consists of sorting the data for the comparison and keeping only emission contributions that are relevant enough. In a second step, the method identifies, among those relevant emissions, the most important differences that provide evidence of methodological divergence and/or errors that can be found and resolved in at least one of the inventories. Although this screen-

ing does not allow checking of the quality of the inventories in an absolute way, the magnitude of the differences is often large enough to make it possible to identify one best value out of the two inventory estimates, even though the truth is unknown.

The approach has been used to compare two versions of the CAMS-REG European-scale inventory over 150 cities in Europe for selected activity sectors. The versions 2.2.1 and 4.2 of this inventory differ both in terms of reporting year (new activity data, new emission factors, etc.) and in terms of spatial distribution (e.g., split in road transport emissions between urban, rural, and highway shares, new proxies for agriculture, etc.). Among the 4500 screened pollutant sectors, about 450 were kept as relevant, among which 46 showed inconsistencies. The analysis indicated that these inconsistencies arose almost equally from reporting by countries and methodological issues in CAMS-REG (e.g., spatial distribution). They mostly affect SO<sub>2</sub> and PM coarse emissions from the industrial and residential sectors. Differences in terms of reporting may be the result of correction of an error and/or the implementation of different methodology to estimate the emissions. But the fact that about half of the inconsistencies can be attributed to changes in country reporting stresses the necessity to further check the informative inventory reports (IIRs) that are submitted annually along with the reported emissions. For inconsistencies related to the CAMS-REG methodology and the spatial distribution therein in particular, the analysis presented here showed that for specific cities, screened errors could be explained and some of them resolved, leading to improved inventories.

Although only a particular example has been discussed here, the screening approach is general and can be used for other types of applications related to emission inventories. The approach can be applied to other inventory scales (e.g., regional or local) and can be tuned to address different sectors or areas. Intensive agriculture or industrial areas could, for example, be added to the urban agglomerations considered in this work. Emission expertise, which is strongly related to a given application (e.g., location, sector), is important in order to analyze the screening results and to correct likely errors. The screening approach also allows assessment of the consistency of a temporal series of emissions, a comparison of inventories based on different sources of information, or even a comparison of inventories based on different methodologies (e.g., comparison of top-down and bottom-up). The latter are the subject of a follow-up paper.

## Appendix A

This section provides details on the cities considered in this study in terms of sectors and emitted pollutants for which a distinction is made between non-relevant, relevant, and inconsistent emission inventory pairs. The table below distin-

guishes between non-relevant and relevant for each city, the latter being further split into consistent and inconsistent.

**Table A1.** Details of the screening output for the 150 cities, 6 emitted pollutants (NH<sub>3</sub>, NMVOC, NO<sub>x</sub>, PM<sub>CO</sub>, PM<sub>2.5</sub>, and SO<sub>2</sub>), and 5 considered sectors (public power, residential, transport, industry, and other). In the table, sectors are represented by their first letter. Empty cells mean that no relevant emissions have been screened. Black letters indicate relevant and consistent emissions, whereas bold letters indicate relevant but inconsistent emissions.

	NH <sub>3</sub>	NMVOC	NO <sub>x</sub>	PM <sub>CO</sub>	PM <sub>2.5</sub>	SO <sub>2</sub>
Cardiff		O			R	
The Hauge		O				
Coruna						I
Alicante		O	T	I	R	
Amsterdam		O	T	I	I	PI
Angers		O	T	I		<b>I</b>
Antwerp						I
Aarhus		O			R	I
Athens		TO		<b>I</b>		I
Augsburg		O		I		
Barcelona		O				
Bari		O	T		R	I
Belfast		O				P
Berlin		O		I		
Bialystok		O	T	R	R	P
Bilbao		O				I
Bologna		O	T	I	R	I
Bonn		O		I		
Bordeaux		O	T	I		<b>I</b>
Bratislava		O	IT		R	
Braunschweig						PI
Bremen		O	T	I		PI
Brescia		O	T	I	R	I
Bristol		O	T			
Brno		<b>OR</b>			<b>R</b>	
Brussels		O	T		R	
Bucharest		O	T	I		I
Budapest		O	T	<b>I</b>	R	R
Burgas			I	I	R	I
Bydgoszcz		O		R	R	P
Caen		O	T	I	R	I
Catania		O	T	I		I
Clermont-F.		O	T	I	R	<b>I</b>
Czestochowa		O	IT	R	IR	
Dresden		O		I		P
Dublin		IO	T	<b>I</b>	R	R
Düsseldorf		O	P	I		PI
Edinburgh		O	T	<b>I</b>	R	
Eindhoven		O	T	I	T	
Florence		O	T		R	I
Frankfurt		O		I		
Freiburg		O	T	I		
Gdansk		O	T	R	R	P
Geneva		O	T			
Genoa			T			P
Gijon						P
Glasgow		O		<b>I</b>		
Gothenburg		IO	T	T		I

Table A1. Continued.

	NH <sub>3</sub>	NMVOC	NO <sub>x</sub>	PM <sub>CO</sub>	PM <sub>2,5</sub>	SO <sub>2</sub>
Graz		O	T	I	R	I
Grenoble		O	T	I	R	I
Hamburg		O		I		I
Hanover		O	T	I		P
Heidelberg		O		I		
Helsinki		O	PT	TI	R	P
Iasi	O	O	T	I	R	PI
Karlsruhe		O		I		PI
Katowice		O	P	I	I	PI
Kiel		O		I		
Kielce		OI		R	R	
Copenhagen		O	T			
Cologne			P			P
Kosice			I	I		I
Krakow		O			R	P
Leeds						P
Lefkosia		O				
Leicester		O	T			
Leipzig						P
Lemesos						P
Liberec		OR			R	
Liege		O	IT	I	R	I
Lille		O	T	I		I
Linz						I
Lisbon		O		I	I	I
Liverpool		O		I		PI
Ljubljana		O	T		R	
Lodz		O	P	R	R	P
London	O	O				
Lublin		O	T	R	R	P
Luxembourg		O	T	T	R	I
Lyon		O	T	I		I
Madrid		O	T			
Malaga		O	T			
Malmö		O	T	T		
Manchester		O	T			
Mannheim		O	I	I		PI
Marseille						I
Metz						P
Milan		O	T			I
Modena		O	T	I	R	I
Montpellier		O	T	I		I
Mulhouse		O	T	I	R	I
Munich		O	T	I		
Nancy						I
Nantes		O	T	I		P
Naples		O	T		R	
Newcastle				I		
Nice		O	T			
Nottingham		O				PI
Nuremberg		O	T	I		
Orleans		O	T	I	R	I
Oslo		O				
Ostrava		OR	PI	IO	R	PI
Oviedo						P

Table A1. Continued.

	NH <sub>3</sub>	NMVOG	NO <sub>x</sub>	PM <sub>CO</sub>	PM <sub>2.5</sub>	SO <sub>2</sub>
Padua		O	T	I	R	I
Palermo		O	T		R	
Palma de M.		O			R	
Paris		O				
Parma		O	T	I	R	I
Plovdiv			I	I	R	
Plzen		O			<b>R</b>	P
Porto		O	T	I		I
Poznan		O		R	R	P
Prague		<b>OR</b>			<b>R</b>	P
Rennes		O	T	I	R	<b>I</b>
Riga		O		<b>I</b>		
Rome		O	T		R	
Rotterdam						I
Rouen		O	<b>TI</b>	I	R	<b>PI</b>
Ruhr				I		I
Rzeszow		O		R	R	
Saarbrücken				I		PI
Santander						PI
Sevilla		O	T		R	
Sheffield		O		<b>I</b>		
Sofia		<b>O</b>	T	I	R	P
Stockholm		O		T		
Strasbourg		O	T	I	R	<b>I</b>
Stuttgart		O		I		
Szczecin		O	P			P
Tallinn		O		I	I	P
Taranto						<b>I</b>
Thessaloniki		O		<b>I</b>	I	
Turin		O	T		R	I
Toulouse		O	T	I		<b>I</b>
Tours		O	T	I	R	
Usti nad Labem						P
Utrecht		O	T		T	
Valencia		O				
Valetta		O	<b>P</b>			P
Varna	I			I		
Venice						P
Verona		O	T		R	I
Vilnius		O	T		<b>R</b>	
Warsaw		O	T	R	R	P
West Midlands urban		O		<b>I</b>		
Vienna		O		I		
Wroclaw		O		R	<b>RI</b>	P
Zagreb		O	T	I	R	P
Zaragoza		O				
Zurich		O	T			

*Code and data availability.* The IDL code and associated input data are archived on Zenodo (<https://doi.org/10.5281/zenodo.5654911>, Thunis, 2021).

*Author contributions.* PT developed the screening approach and wrote most of the text. EP prepared and formatted the input emission data and contributed to the text. AC contributed to the methodological aspects and contributed to the writing on this. JK contributed to the analysis of the results and provided text on this. BB, SLA, and MG reviewed and contributed to the text.

*Competing interests.* The contact author has declared that none of the authors have any competing interests.

*Disclaimer.* Publisher's note: Copernicus Publications remains neutral with regard to jurisdictional claims in published maps and institutional affiliations.

*Review statement.* This paper was edited by Havala Pye and reviewed by two anonymous referees.

## References

- Britz, W. and Witzke, P.: CAPRI Model Documentation 2014, [https://www.capri-model.org/dokuwiki\\_help/](https://www.capri-model.org/dokuwiki_help/) (last access: 1 July 2022), 2015.
- Clappier, A. and Thunis, P.: A probabilistic approach to screen and improve emission inventories, *Atmos. Environ.*, 242, 117831, <https://doi.org/10.1016/j.atmosenv.2020.117831>, 2020.
- Crippa, M., Guizzardi, D., Muntean, M., Schaaf, E., Dentener, F., van Aardenne, J. A., Monni, S., Doering, U., Olivier, J. G. J., Pagliari, V., and Janssens-Maenhout, G.: Gridded emissions of air pollutants for the period 1970–2012 within EDGAR v4.3.2, *Earth Syst. Sci. Data*, 10, 1987–2013, <https://doi.org/10.5194/essd-10-1987-2018>, 2018.
- Cuvelier, C., Thunis, P., Vautard, R., Amann, A., Bessagnet, B., Bedogni, M., Berkowicz, R., Brandt, J., Brocheton, F., Bultjes, P., Carnavale, C., Coppalle, A., Denby, B., Douros, J., Graf, A., Hellmuth, O., Hodzic, A., Honore, C., Jonson, J., Kerschbaumer, A., de Leeuw, F., Minguzzi, E., Moussiopoulos, N., Pertot, C., Peuch, V. H., Pirovano, G., Rouil, L., Sauter, F., Schaap, M., Stern, R., Tarrason, L., Vignati, E., Volta, M., White, L., Wind, P., and Zuber, A.: CityDelta: A model intercomparison study to explore the impact of emission reductions in European cities in 2010, *Atmos. Environ.* 41, 189–207, 2007.
- de Meij, A., Gzella, A., Cuvelier, C., Thunis, P., Bessagnet, B., Vinuesa, J. F., Menut, L., and Kelder, H. M.: The impact of MM5 and WRF meteorology over complex terrain on CHIMERE model calculations, *Atmos. Chem. Phys.*, 9, 6611–6632, <https://doi.org/10.5194/acp-9-6611-2009>, 2009.
- de Meij, A., Zittis, G., and Christoudias, T.: On the uncertainties introduced by land cover data in high-resolution regional simulations, *Meteorol. Atmos. Phys.*, 131, 1213–1223, <https://doi.org/10.1007/s00703-018-0632-3>, 2018.
- Dufour, G., Hauglustaine, D., Zhang, Y., Eremenko, M., Cohen, Y., Gaudel, A., Siour, G., Lachatre, M., Bense, A., Bessagnet, B., Cuesta, J., Ziemke, J., Thouret, V., and Zheng, B.: Recent ozone trends in the Chinese free troposphere: role of the local emission reductions and meteorology, *Atmos. Chem. Phys.*, 21, 16001–16025, <https://doi.org/10.5194/acp-21-16001-2021>, 2021.
- European Environment Agency (EEA): Air Quality in Europe: 2020 Report, Publications Office, (CSL JSON), <https://doi.org/10.2800/786656>, 2020.
- Geng, G., Zhang, Q., Martin, R. V., Lin, J., Huo, H., Zheng, B., Wang, S., and He, K.: Impact of spatial proxies on the representation of bottom-up emission inventories: A satellite-based analysis, *Atmos. Chem. Phys.*, 17, 4131–4145, <https://doi.org/10.5194/acp-17-4131-2017>, 2017.
- Im, U., Christensen, J. H., Geels, C., Hansen, K. M., Brandt, J., Solazzo, E., Alyuz, U., Balzarini, A., Baro, R., Bellasio, R., Bianconi, R., Bieser, J., Colette, A., Curci, G., Farrow, A., Flemming, J., Fraser, A., Jimenez-Guerrero, P., Kitwiroon, N., Liu, P., Nopmongkol, U., Palacios-Peña, L., Pirovano, G., Pozzoli, L., Prank, M., Rose, R., Sokhi, R., Tuccella, P., Unal, A., Vivanco, M. G., Yarwood, G., Hogrefe, C., and Galmarini, S.: Influence of anthropogenic emissions and boundary conditions on multi-model simulations of major air pollutants over Europe and North America in the framework of AQMEII3, *Atmos. Chem. Phys.*, 18, 8929–8952, <https://doi.org/10.5194/acp-18-8929-2018>, 2018.
- Jalkanen, J.-P., Brink, A., Kalli, J., Pettersson, H., Kukkonen, J., and Stipa, T.: A modelling system for the exhaust emissions of marine traffic and its application in the Baltic Sea area, *Atmos. Chem. Phys.*, 9, 9209–9223, <https://doi.org/10.5194/acp-9-9209-2009>, 2009.
- Kryza, M., Jóźwicka, M., Dore, A. J., and Werner, M.: The uncertainty in modelled air concentrations of NO<sub>x</sub> due to choice of emission inventory, *Int. J. Environ. Pollut.*, 57, 3–4, 2015.
- Kuenen, J., Dellaert, S., Visschedijk, A., Jalkanen, J.-P., Super, I., and Denier van der Gon, H.: CAMS-REG-v4: a state-of-the-art high-resolution European emission inventory for air quality modelling, *Earth Syst. Sci. Data*, 14, 491–515, <https://doi.org/10.5194/essd-14-491-2022>, 2022.
- Markakis, K., Valari, M., Perrussel, O., Sanchez, O., and Honore, C.: Climate-forced air-quality modeling at the urban scale: sensitivity to model resolution, emissions and meteorology, *Atmos. Chem. Phys.*, 15, 7703–7723, <https://doi.org/10.5194/acp-15-7703-2015>, 2015.
- Ramacher, M. O. P., Kakouri, A., Speyer, O., Feldner, J., Karl, M., Timmermans, R., Denier van der Gon, H., Kuenen, J., Gerasopoulos, E., and Athanasopoulou, E.: The UrbEm Hybrid Method to Derive High-Resolution Emissions for City-Scale Air Quality Modeling, *Atmosphere*, 12, 1404, <https://doi.org/10.3390/atmos12111404>, 2021.
- Thunis, P.: A multi-pollutant and multi-sectorial approach to screen the consistency of emission inventories, Zenodo [code], <https://doi.org/10.5281/zenodo.5654911>, 2021.
- Thunis, P., Rouil, L., Cuvelier, C., Stern, R., Kerschbaumer, A., Bessagnet, B., Schaap, M., Bultjes, P., Tarrason, L., Douros, J., Moussiopoulos, N., Pirovano, G., and Bedogni, M.: Analysis of model responses to emission-reduction scenarios within the City-Delta project, *Atmos. Environ.*, 41, 208–220, 2007.

- Thunis, P., Degraeuwe, B., Cuvelier, C., Guevara, M., Tarrason, L., and Clappier, A.: A novel approach to screen and compare emission inventories, *Air Qual. Atmos. Health*, 9, 325–333, 2016.
- Thunis, P., Degraeuwe, B., Pisoni, E., Trombetti, M., Peduzzi, E., Belis, C. A., Wilson, J., Clappier, A., and Vignati, E.: PM<sub>2.5</sub> source allocation in European cities: A SHERPA modelling study, *Atmos. Environ.*, 187, 93–106, 2018.
- Trombetti, M., Thunis, P., Bessagnet, B., Clappier, A., Couvidat, F., Guevara, M., Kuenen, J., and López-Aparicio, S.: Spatial inter-comparison of Top-down emission inventories in European urban areas, *Atmos. Environ.*, 173, 142–156, 2018.
- Zhang, W., Trail, M. A., Hu, Y., Nenes, A., and Russell, A. G.: Use of high-order sensitivity analysis and reduced-form modeling to quantify uncertainty in particulate matter simulations in the presence of uncertain emissions rates: A case study in Houston, *Atmos. Environ.*, 122, 103–113, 2015.
- Zheng, B., Cheng, J., Geng, G., Wang, X., Li, M., Shi, Q., Qi, J., Lei, Y., Zhang, Q., and He, K.: Mapping anthropogenic emissions in China at 1 km spatial resolution and its application in air quality modeling, *Sci. Bull.*, 66, 612–620, 2021.
- Zhu, S., Kinnon, M. M., Shaffer, B. P., Samuelsen, G. S., Brouwer, J., and Dabdub, D.: An uncertainty for clean air: Air quality modeling implications of underestimating VOC emissions in urban inventories, *Atmos. Environ.*, 211, 256–267, 2019.